J. Am. Chem. Soc. 1988, 110, 15-24

Hydrocarbon Activation by Gas-Phase Lanthanide Cations: Interaction of Pr$^+$, Eu$^+$, and Gd$^+$ with Small Alkanes, Cycloalkanes, and Alkenes

J. Bruce Schilling and J. L. Beauchamp*

Contribution No. 7590 from the Arthur Amos Noyes Laboratory of Chemical Physics, California Institute of Technology, Pasadena, California 91125. *Received May 18, 1987*

Abstract: We describe ion beam studies of the interaction of gas-phase lanthanide ions, praseodymium (Pr$^+$), europium (Eu$^+$), and gadolinium (Gd$^+$), with small alkanes, cycloalkanes, alkenes, and several oxygen-containing compounds. Only Gd$^+$ is seen to activate C–H and C–C bonds of alkanes. The ground-state electronic configuration of Gd$^+$ (4f^{7}5d^{1}6s^1) is different from those of Pr$^+$ (4f^{3}6s^1) and Eu$^+$ (4f^{7}6s^1), leading to the conclusion that the f electrons play little part in the metal ion reactivity. Gd$^+$ can be thought of as having two valence electrons, and indeed it reacts similarly to Sc$^+$ and the other group 3 metal ions Y$^+$ and La$^+$, yielding products corresponding to elimination of hydrogen, alkanes, and alkenes. The elimination of neutral alkenes in the reaction of Gd$^+$ with alkanes results in the formation of metal dialkyl or hydrido-alkyl complexes. This finding leads to estimates for the sum of two Gd$^+$ σ bond dissociation energies of between 110 and 130 kcal/mol. Gd$^+$ and Pr$^+$ react readily with alkenes, yielding mostly dehydrogenation products along with smaller amounts of C–C bond cleavage products. Reactions of Gd$^+$ and Pr$^+$ with oxygen-containing species such as nitric oxide, formaldehyde, acetaldehyde, and acetone yield primarily the metal oxide ions and provide a lower limit for D(M$^+$–O) of 179 kcal/mol, in good agreement with literature values of D(Pr$^+$–O) = 188.4 ± 5.2 kcal/mol and D(Gd$^+$–O) = 181.0 ± 4.4 kcal/mol. In keeping with the strong metal σ bonds, Gd$^+$ is also seen to readily react with formaldehyde to eliminate CO and form GdH$_2$$^+$.

Studies of gas-phase atomic transition metal ions have shown that many of these systems are very reactive in the activation of both C–H and C–C bonds in small alkanes, cycloalkanes, alkenes, and other organic molecules. While studies have expanded to include most of the first[1-6] and second[7-9] row metals and a few of the third row transition series,[9-11] the reactivity of many of the heavier metals is still unknown. Both experimental[12] and theoretical[13-15] studies are gradually detailing the types of metal orbitlas necessary to form strong metal ion–ligand bonds as well as the electronic structures best suited for activation of C–C and C–H bonds.

To further these basic investigations, the present paper details experiments involving three lanthanide ions, praseodymium (Pr$^+$), europium (Eu$^+$), and gadolinium (Gd$^+$), which show a wide range of reactivity. The intent of the present study was to examine the role of f orbitals in the reactivity of the metal ions with organic molecules. Although the reactions of La$^+$ with hydrocarbons have recently been described,[9] no systematic gas-phase studies of the bare lanthanide series ions have been reported. Solution-phase results for various Cp$^*_2$MCH[Si(CH$_3$)$_3$]$_2$ and [Cp$^*_2$MH]$_2$ (Cp* = pentamethylcyclopentadiene; M = La, Nd, Sm, and Lu)[16] species along with Cp$^*_2$LuCH$_3$[17] have shown that these lanthanide complexes are very active ethylene polymerization catalysts. The Cp$^*_2$LuCH$_3$ species has also been shown to activate a variety of C–H bonds including alkyl–H, phenyl–H, benzyl–H, vinyl–H, and even the C–H bonds in methane.[17]

Table I. Selected Ionic Radii[a]

ion	state	confign	R_s[b] (Å)	R_d[c] (Å)
Sc$^+$	^{3}D	3d^{1}4s^1	2.02	1.01
Ti$^+$	^{4}F	3d^{2}4s^1	1.89	0.87
Y$^+$	^{3}D	4d^{1}5s^1	2.14	1.38
Zr$^+$	^{4}F	4d^{2}5s^1	2.00	1.21
La$^+$	^{3}D	5d^{1}6s^1	2.38	1.59
Hf$^+$	^{4}F	5d^{2}6s^1	1.90	1.30

[a] Root-mean-square radii from Hartree–Fock calculations on the atomic ions, taken from ref 13. [b] R_s is the radius of the valence s orbital. [c] R_d is the radius of the valence d_{z^2} orbital.

The most common ground-state valence electronic structure of the lanthanide cations is 4f^{n-1}6s^1, where n is the total number of valence electrons.[18] Ce$^+$ (4f^{1}5d^2), Gd$^+$ (4f^{7}5d^{1}6s^1), and Lu$^+$ (4f^{14}6s^2) are exceptions to this. We have chosen two metal ions, Pr$^+$ (4f^{3}6s^1) and Eu$^+$ (4f^{7}6s^1), with the standard lanthanide configuration, one with three f electorns and one with a half-full f shell. The f orbitals of the heavier lanthanides would be expected to participate *less* in bonding to hydrogen or carbon owing to the orbital contraction which occurs in moving from left to right along the row (the f orbitals contract faster than the 5d and 6s orbitals). The effects of the so-called "lanthanide contraction" can be seen by the examining the size of the orbitals of La$^+$ and Hf$^+$, as shown in Table I. We have also chosen to study Gd$^+$ which has a

---

(1) Tolbert, M. A.; Beauchamp, J. L. *J. Am. Chem. Soc.* **1984**, *106*, 8117.

(2) Tolbert, M. A.; Beauchamp, J. L. *J. Am. Chem. Soc.* **1986**, *108*, 7508.

(3) Byrd, G. D.; Burnier, R. C.; Freiser, B. S. *J. Am. Chem. Soc.* **1982**, *104*, 3565.

(4) (a) Halle, L. F.; Armentrout, P. B.; Beauchamp, J. L. *Organometallics* **1982**, *1*, 963. (b) Houriet, R.; Halle, L. F.; Beauchamp, J. L. *Ibid.* **1983**, *2*, 1818. (c) Jacobson, D. B.; Freiser, B. S. *J. Am. Chem. Soc.* **1983**, *105*, 5197.

(5) (a) Armentrout, P. B.; Halle, L. F.; Beauchamp, J. L. *J. Am. Chem. Soc.* **1981**, *103*, 6624. (b) Jacobson, D. B.; Freiser, B. S. *Ibid.* **1983**, *105*, 7484. (c) Peake, D. A.; Gross, M. L.; Ridge, D. P. *Ibid.* **1984**, *106*, 4307.

(6) (a) Armentrout, P. B.; Beauchamp, J. L. *J. Am. Chem. Soc.* **1981**, *103*, 6628. (b) Jacobson, D. B.; Freiser, B. S. *Ibid.* **1983**, *105*, 7492.

(7) Tolbert, M. A.; Mandich, M. L.; Halle, L. F.; Beauchamp, J. L. *J. Am. Chem. Soc.* **1986**, *108*, 5675.

(8) Byrd, G. D.; Freiser, B. S. *J. Am. Chem. Soc.* **1982**, *104*, 5944.

(9) Huang, Y.; Wise, M. B.; Jacobson, D. B.; Freiser, B. S. *Organometallics* **1987**, *6*, 346.

(10) (a) Wise, M. B.; Jacobson, D. B.; Freiser, B. S. *J. Am. Chem. Soc.* **1985**, *107*, 1590. (b) Wise, M. B.; Jacobson, D. B.; Freiser, B. S. *Ibid.* **1985**, *107*, 6744.

(11) Weil, D. A.; Wilkins, C. L. *J. Am. Chem. Soc.* **1985**, *107*, 7316.

(12) Armentrout, P. B. In *Structure/Reactivity and Thermochemistry of Ions*, Ausloos, P. J., Lias, S. G. Eds. (NATO ASI Series C); Reidel: Dordrecht, 1987, and references therein.

(13) (a) Schilling, J. B.; Beauchamp, J. L.; Goddard, W. A., III *J. Am. Chem. Soc.* **1986**, *108*, 582. (b) Schilling, J. B.; Beauchamp, J. L.; Goddard, W. A., III *J. Am. Chem. Soc.* **1987**, *109*, 5565. (c) Schilling, J. B.; Beauchamp, J. L.; Goddard, W. A., III *J. Am. Chem. Soc.* **1987**, *109*, 5573. (d) Schilling, J. B.; Goddard, W. A., III; Beauchamp, J. L. *J. Phys. Chem.* **1987**, *91*, 4470.

(14) (a) Carter, E. A.; Goddard, W. A., III *J. Phys. Chem.* **1984**, *88*, 1485. (b) Carter, E. A.; Goddard, W. A., III *J. Am. Chem. Soc.* **1986**, *108*, 2180. (c) Carter, E. A.; Goddard, W. A., III *Ibid.* **1986**, *108*, 4746.

(15) (a) Alvarado-Swaisgood, A. E.; Allison, J.; Harrison, J. F. *J. Phys. Chem.* **1985**, *89*, 2517. (b) Alvarado-Swaisgood, A. E.; Harrison, J. F. *Ibid.* **1985**, *89*, 5198. (c) Mavridis, A.; Alvarado-Swaisgood, A. E.; Harrison, J. F. *J. Phys. Chem.* **1986**, *90*, 2584. (d) Harrison, J. F. *Ibid.* **1986**, *90*, 3313.

(16) (a) Jeske, G.; Lauke, H.; Mauermann, H.; Swepston, P. N.; Schumann, H.; Marks, T. J. *J. Am. Chem. Soc.* **1985**, *107*, 8091. (b) Jeske, G.; Schock, L. E.; Swepston, P. N.; Schumann, H.; Marks, T. J. *Ibid.* **1985**, *107*, 8103. (c) Jeske, G.; Lauke, H.; Mauermann, H.; Schumann, H.; Marks, T. J. *Ibid.* **1985**, *107*, 8111.

(17) Watson, P. L.; Parshall, G. W. *Acc. Chem. Res.* **1985**, *18*, 51, and references therein.

(18) Martin, W. C.; Zalubas, R.; Hagan, L. *Atomic Energy Levels-The Rare-Earth Elements*; National Bureau of Standards: Washington, D.C., 1978.

0002-7863/88/1510-0015$01.50/0

Table II. Low-Lying M$^+$ Electronic States[a] and Beam Populations

ion	confign	term	E_{rel}(low J)[b] (eV)	E_{rel}(av J)[c] (eV)	ion beam population[d] (%)
Eu$^+$	$\mathrm{4f^76s^1}$	$\mathrm{a^9S^0}$	0.00	0.00	78.07
	$\mathrm{4f^76s^1}$	$\mathrm{a^7S^0}$	0.21	0.21	21.37
	$\mathrm{4f^75d^1}$	$\mathrm{a^9D^0}$	1.23	1.31	0.55
	$\mathrm{4f^75d^1}$	$\mathrm{a^7D^0}$	2.09	2.11	0.01
	$\mathrm{4f^76p^1_{1/2}}$	(7/2, 1/2)	2.95	2.98	0.00
	$\mathrm{4f^76p^1_{3/2}}$	(7/2, 3/2)	3.24	3.31	0.00
Gd$^+$	$\mathrm{4f^75d^16s^1}$	$\mathrm{^{10}D^0}$	0.00	0.00	78.64
	$\mathrm{4f^75d^16s^1}$	$\mathrm{^8D^0}$	0.35	0.36	10.38
	$\mathrm{4f^76s^2}$	$\mathrm{^8S^0}$	0.43	0.30	2.47
	$\mathrm{4f^75d^2}$	$\mathrm{^{10}F^0}$	0.50	0.55	7.33
	$\mathrm{4f^86s^1}$	$\mathrm{^8F}$	0.99	1.11	0.44
	$\mathrm{4f^75d^16s^1}$	$\mathrm{^8D^0}$	1.06	0.99	0.40
	$\mathrm{4f^86s^1}$	$\mathrm{^6F}$	1.23	1.33	0.10
	$\mathrm{4f^75d^16s^1}$	$\mathrm{^6D^0}$	1.25	1.17	0.12
	$\mathrm{4f^75d^2}$	$\mathrm{^{10}P^0}$	1.31	1.26	0.08
	$\mathrm{4f^75d^2}$	$\mathrm{^8F^0}$	1.57	1.52	0.04
Pr$^+$	$\mathrm{4f^36s^1_{1/2}}$	$(9/2, 1/2)^0$	0.00	0.00	46.50
	$\mathrm{4f^36s^1_{1/2}}$	$(11/2, 1/2)^\circ$	0.20	0.18	22.34
	$\mathrm{4f^36s^1_{1/2}}$	$(13/2, 1/2)^0$	0.37	0.36	10.31
	$\mathrm{4f^35d^1}$	$\mathrm{^5L^0}$	0.48	0.81	6.08
	$\mathrm{4f^35d^1}$	$\mathrm{^5K^0}$	0.51	0.81	4.89
	$\mathrm{4f^36s^1_{1/2}}$	$(15/2, 1/2)^0$	0.55	0.56	4.52
	$\mathrm{4f^25d^2}$	$\mathrm{^5L}$	0.73	0.70	0.89
	$\mathrm{4f^25d^2}$	$\mathrm{^5I}$	0.90	0.87	0.26
	$\mathrm{4f^35d^1}$	$\mathrm{^3I^0}$	0.92	0.96	0.46
	$\mathrm{4f^35d^1}$	$\mathrm{^5I^0}$	0.92	1.21	0.53
	$\mathrm{4f^35d^1}$	$\mathrm{^5H}$	0.96	1.22	0.44

[a] Electronic state information taken from ref 18. [b] Relative energy determined using the splitting between the lowest *j* level for each state. [c] Relative energy determined using a weighted average over *j* levels for each state. [d] Populations determined using a maxwell–Boltzman distribution over the energy levels at a temperature of 2300 K.

half-full f shell and two non-f valence orbitals. Reactivity differences in these three metal ions should serve to detail the possible role of f electrons in the activation of small molecules by lanthanide ions.

Experimental Details

The ion beam apparatus has been described previously.[19] Briefly, bare metal cations are produced in the source as described below. The ions are accelerated, collimated into an ion beam, mass and energy selected, and injected into a collision cell holding a neutral reactant gas. The gas is at ambient temperature and is held at a constant pressure of 2 mtorr or less. This pressure range allows study of the reactions under single-collision conditions. Product ions scattered in the forward direction as well as unreacted metal ions are extracted from the collision cell and injected into a quadrupole mass spectrometer. The mass selected ions are then detected using a conversion dynode coupled with a channeltron electron multiplier. Ion counting as well as quadrupole control are achieved using an IBM-PC XT computer.

The metal ions in this study were produced by the process of surface ionization. A metal salt is heated in a small oven to ~650 °C, vaporized onto a hot rhenium ribbon filament, and surface ionized at a temperature between 2200 and 2400 K. The metal salts used in the present study were the metal trichlorides for all three of the metals studied. Praseodymium chloride was purchased as an anhydrous salt while the other two metal chlorides were obtained as hydrates. The two hydrates were placed in an oven at 120 °C for several hours before use.

It is generally assumed that the ions resulting from surface ionization have an internal temperature equivalent to the surface temperature of the filament. A Maxwell–Boltzmann distribution over electronic energy levels thus gives an approximate distribution of the ions in the ground and low-lying excited electronic states. Table II presents some of the low-lying electronic states for the three metal ions, Pr$^+$, Eu$^+$, and Gd$^+$, along with the state splittings and an estimate of the beam population at a temperature of 2300 K. For Eu$^+$, only three states are present in any significant amount. The $\mathrm{a^9S^\circ}$ ($\mathrm{4f^76s^1}$) and $\mathrm{a^7S^\circ}$ ($\mathrm{4f^76s^1}$) states amount to over 99% of the beam while the $\mathrm{a^9D^\circ}$ ($\mathrm{4f^75d^1}$) state accounts for over 0.5%. For Gd$^+$, a few more states contribute to the overall population of the beam. The $\mathrm{^{10}D^\circ}$ and $\mathrm{^8D^\circ}$ states ($\mathrm{4f^75d^16s^1}$) make up approximately 89% of the beam, while $\mathrm{^{10}F^\circ}$ ($\mathrm{4f^75d^2}$, 7.3%) and $\mathrm{^8S^\circ}$ ($\mathrm{4f76s^2}$, 2.5%) are the other significant contributors to the remainder. Pr$^+$ has a large number of low-lying electronic excited states. Table II, which is by no means a complete list of electronic states represented in the beam, lists some of the more significant levels. It is likely that reactions of excited states will be observed in the experiments involving Pr$^+$. Products corresponding to metal oxide ions were observed for all three metal ions. These result from exothermic reactions with background oxygen (O_2, H_2O) sources in the collision chamber.

Table III. Adduct Formation in the Reactions of Pr$^+$ with Alkanes

alkane	apparent adduct cross section[a] (Å^2)
propane	0.00
n-butane	0.04
2-metyhylpropane	0.06
n-hexane	0.26
2,3-dimethylbutane	0.59
n-heptane	2.46
2,4-dimethylpentane	2.33

[a] From experiments at a center-of-mass collision energy of ~0.25 eV and neutral pressures between 1.2 and 1.6 mtorr.

Results and Discussion

Interaction of Eu$^+$ and Pr$^+$ with Alkanes and Cycloalkanes. We have looked at the low-energy interaction (<1 eV in the center-of-mass) of praseodymium and europium ions with a number of alkanes including propane, *n*-butane, and 2-methylpropane. Pr$^+$ was also studied with hexane, 2,3-dimethylbutane, heptane, and 2,4-dimethylpentane. With Eu$^+$, no reaction products are observed in the three cases examined. In addition, only very small amounts of adduct are observed (at maximum pressures which are lower than 2 mtorr). The praseodymium ion is also seen to be quite unreactive with all of the alkanes studied, although very small amounts of multiple hydrogen loss products are seen at low energies for almost all of the species. The product reaction cross sections are, however, all much less than 1 Å^2. The cross section vs. energy data tend to indicate that there is a very small amount of product formed exothermically and to this is added endothermic processes as the energy is increased. The extremely low apparent cross sections for what appear to be exothermic processes indicate that the reactivity is probably due to one or more of the excited states in the Pr$^+$ beam.

Pr$^+$ has also been reacted with the cyclic alkanes, cyclopropane, cyclobutane, and cyclohexane. Cyclopropane reacts with Pr$^+$ to form two products $\mathrm{Pr(C_3H_4)^+}$ and $\mathrm{PrCH_2^+}$, both of which appear to be formed in endothermic processes with threshold energies below 0.25 eV. Reaction of Pr$^+$ with cyclohexane also shows a slightly endothermic reaction, the elimination of three molecules of H_2 and formation of $\mathrm{Pr(C_6H_6)^+}$ (presumably a Pr$^+$–benzene complex). Reaction with cyclobutane produces $\mathrm{Pr(C_4H_6)^+}$ in what is apparently an exothermic reaction. Since the apparent cross section at a collision energy of 0.25 eV is only 2.4 Å^2, it is again possible that this product is formed by reaction of Pr$^+$ excited states. A second product, $\mathrm{Pr(C_4H_4)^+}$, is also observed but with endothermic behavior.

The only cyclic alkane that we have studied with Eu$^+$ is cyclopropane, expected to be one of the more reactive of the cycloalkanes owing to its highly strained nature and weak C–C bonds. As with the linear alkanes, no reaction products are observed. Thus, both Eu$^+$ and Pr$^+$ are quite unreactive with cycloalkanes.

There are several possible explanations for the unreactive behavior of Pr$^+$ and Eu$^+$ with the smaller alkanes and cycloalkanes. The first step in a gas-phase ion–molecule reaction is presumably formation of a loose collision complex held together by interaction of the ion with either a permanent dipole or an ion-induced dipole. Adduct formation may result if the interaction of the metal ion and neutral results in the formation of a complex which is sufficiently long-lived to undergo a stabilizing collision with another neutral gas molecule. In the Pr$^+$ experiments, the amount of adduct is seen to increase with the increasing size of the neutral hydrocarbon (Table III), consistent with an increase of the neutral polarizability and the subsequent increase in the ion-induced dipole interaction with the metal ion. It is the chemical activation gained

---

(19) (a) Armentrout, P. B.; Beauchamp, J. L. *Chem. Phys.* **1980**, *50*, 21. (b) Armentrout, P. B.; Beauchamp, J. L. *J. Chem. Phys.* **1981**, *74*, 2819.

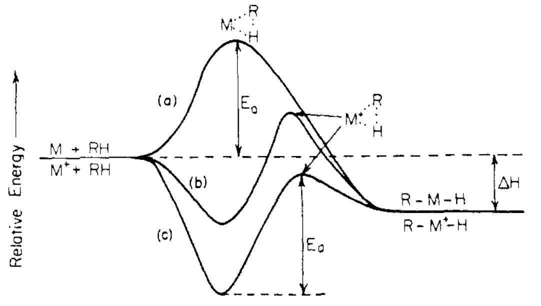

Figure 1. Illustration of the effects of chemical activation in ion–molecule reactions, using a hypothetical insertion of either a neutral metal or metal ion into a C–H bond. Path a shows the neutral reaction with an activation barrier, E_a. Path c shows the effects of the interaction of the ionic charge with an induced dipole in the neutral, effectively lowering the barrier below the total energy of the reactants. Path b represents the situation when the chemical activation is not large enough to effectively overcome the activation barrier.

from this ion–molecule association which allows many ion–molecule reactions to proceed with no appreciable barrier to reaction. This is illustrated in Figure 1. Curve a shows a hypothetical interaction between a neutral metal and alkane and an activation barrier, E_a, for the insertion process. Curve c shows the same insertion process for a metal ion, where we assume that the barrier height remains constant. This barrier height is now measured with respect to the energy of the collision complex, $M(RH)^+$, which is lower in energy than the reactants owing to the ion–molecule interaction energy. This chemical activation lowers the effective barrier to below the total energy of the reacting molecules, allowing the ion–molecule reaction to proceed as if no barrier existed. The early third row metals are fairly large (Table I). An estimate for the size of Eu^+ is given by averaging the 6s orbital sizes of La^+ and Hf^+, giving 2.14 Å. Pr^+ would be expected to be closer to the size of La^+. Since the energy of association is due to electrostatic interactions, one might expect that for a large ion such as Pr^+ or Eu^+, the ion–neutral distance could be such that the energy lowering is not enough to decrease the barrier height to below the total energy of the system (a case such as this is shown as curve b in Figure 1).

For the C–H insertion process to be feasible, the sum of the M^+–C and M^+–H bond dissociation energies must of necessity be larger than the bond energy of the C–H bond being broken. Since almost all of the low-lying electronic states represented in the beam (for Pr^+ and Eu^+) have either an $4f^{n-1}6s^1$ or $4f^{n-1}5d^1$ valence electronic configuration, one of the metal σ bonds must be made with a 4f electron. There are several drawbacks to bonding to f orbitals. First, the 4f orbitals are quite small and compact spatially when compared to the 5d and 6s orbitals. This is due to the lower principal quantum number of the f orbitals (making access to the orbitals difficult). Second, the six-lobed nature of the f orbitals could lower the strength of σ bonds owing to the smaller amount of electron density along any one bond axis (the f_{z^3} orbital would prove best for forming σ bonds just as the d_{z^2} orbital is best of the d orbitals for forming σ bonds).[20] Third, as the number of high-spin coupled f electrons increases, bond energies will decrease owing to the loss of high-spin exchange energy between the electrons. Effects of this type are seen for the first row transition metals where the bonding choice is between the 4s orbital and the much smaller 3d orbitals. Bonding is preferentially to the s orbital, especially in the later metals which have very compact d orbitals.[13] Weak bonds are seen to metals such as Cr^+ (^6S, d^5) where ~36 kcal/mol of exchange energy is lost on bonding to one of the d electrons. Similar effects, possibly even more pronounced, should be expected with the lanthanides. Thus, because of the nature of the f orbitals, one would not expect strong M^+–H or M^+–C bonds to be formed using electrons in these metal orbitals. Also, backbonding between f orbitals and σ* or π* orbitals would not be expected. Although one strong bond can possibly be formed to an s or d orbital, without the formation of two strong metal σ bonds, the oxidative addition of a C–H bond cannot take place and the metal ion will be seen to be unreactive. Higher energy states of the metals with more than one non-f valence electron should be reactive since they no longer must depend on forming a strong bond with an f electron.

Reactions of Gd^+ with Alkanes. Gadolinium ions form a striking contrast to the other two lanthanides, praseodymium and europium. While Pr^+ and Eu^+ are both very unreactive, Gd^+ is quite reactive with alkanes and shows a fairly wide spectrum of products, including activation of both C–H and C–C bonds with the elimination of hydrogen, alkanes, and alkenes. Table IV lists the products, product distributions, and total reaction cross sections for the reaction of Gd^+ with C_1–C_6 alkanes. The reactivity of Gd^+ and the recently observed reactivity of La^+ helps to answer the question of why Pr^+ and Eu^+ are unreactive. Clearly, all of these ions are similar in size and thus a lowering of the ion–molecule association energy cannot totally explain the unreactivity. The very small amount of adduct ions formed by the unreactive ions tends to indicate that the adducts are not very long-lived (possibly indicating a small interaction energy); however, the *larger* La^+ ion *is* reactive. We thus conclude that the difference in reactivity is due to the fact that Gd^+ possesses two non-4f valence electrons and thus does not need to form σ bonds utilizing f electrons. The $4f^7$ shell of electrons probably has little to do with the ion reactivity. Gd^+ can thus be considered to possess a valence electron configuration with two electrons (s^1d^1), very similar to the group 3 metal ions, Sc^+, Y^+, and La^+. We have included the reaction product distributions for these three metals in Table IV.

a. Methane, Ethane, and Propane. Gadolinium follows the general trend of the transition metals in its unreactivity toward methane. Gd^+ does, however, react with ethane, allthough the reaction cross section is small (0.96 Å^2 at a collision energy of 0.09 eV). Two products are observed, as indicated in reactions 1 and 2. These are suggested to be the single and double dehydrogenation products Gd^+–ethylene and Gd^+–acetylene, indicating that the bond energies for the two are greater than or equal to 33 and 75 kcal/mol, respectively.[21]

$$Gd^+ + C_2H_6 \xrightarrow{62\%} Gd(C_2H_4)^+ + H_2 \quad (1)$$

$$\xrightarrow{38\%} Gd(C_2H_2)^+ + 2H_2 \quad (2)$$

Gd^+ is more reactive with propane than with ethane (a total reaction cross section of 6.2 Å^2 at a collision energy of 0.25 eV vs. 0.3 Å^2 for ethane at the same energy). Again, products are seen which correspond to loss of both one and two molecules of H_2, $Gd(C_3H_6)^+$, and $Gd(C_3H_4)^+$. The latter may be either a propyne or allene complex. Formation of propyne and allene from propane is endothermic by 69.2 and 70.5 kcal/mol, respectively. Reaction with propane-*2,2-d*$_2$ (Table V) yields an almost statistical ratio of H_2, HD, and D_2 loss products, indicating very rapid scrambling of the hydrogen atoms. In addition to the two hydrogen loss products, Gd^+–ethylene is formed via elimination of methane. This process can take place either through initial insertion into a terminal C–H bond followed by β-CH_3 transfer and reductive elimination of CH_4 or through initial C–C insertion followed by β-H transfer and methane elimination. With the labeled propane, an almost equal amount of CH_4 and CH_3D loss products is observed. Again, this indicates that some scrambling is taking place since the two mechanisms above predict loss of only CH_4.

As pointed out in the Experimental Details section, GdO^+ is formed in a reaction with the background oxygen. With normal propane, this obscures any $Gd(CH_4)^+$ product formed. Experiments using propane-*d*$_8$ show formation of $GdCD_4^+$. Reaction with propane-*2,2-d*$_2$ yields a 2.3:1 ratio of $GdCDH_3^+$ and $GdCD_2H_2^+$. Any $GdCH_4^+$ product is obscured by the GdO^+ peak.

---

(20) Steigerwald, M. L. Ph.D. Thesis, California Institute of Technology, Pasadena, Calif., 1984.

(21) Heat of formation values for stable organic molecules obtained from: Cox, J. D.; Pilcher, G. *Thermochemistry of Organic and Organometallic Compounds*; Academic Press: New York, 1970.

Table IV. Product Distributions for the Reactions of Gd^+ and Group 3 M^+ with Alkanes

	total reaction cross section (Å^2)^a				relative product intensities (%)				
					ion beam		FTMS^c		
alkane	Gd^+	Sc^{+b}	neutral(s) lost	product ion	Gd^+	Sc^{+b}	Sc^+	Y^+	La^+
CH_4			NR^d	NR^d					
C_2H_6	0.3	1.4	H_2	$M(C_2H_4)^+$	62		71	100	100
			$2H_2$	$M(C_2H_2)^+$	38		29		
C_3H_8^{f}	6	11	H_2	$M(C_3H_6)^+$	68	68	73	75	85
			$2H_2$	$M(C_3H_4)^+$	4	5		25	15
			CH_4	$M(C_2H_4)^+$	28	27	27		
n-C_4H_{10}	110	151	H_2	$M(C_4H_8)^+$	34	44	54	12	4
			$2H_2$	$M(C_4H_6)^+$	27	16	16	47	77
			$3H_2$	$M(C_4H_4)^+$	tr^e				
			CH_4	$M(C_3H_6)^+$	tr^e	2			
			CH_4,H_2	$M(C_3H_4)^+$	tr^e	2	2	3	
			C_2H_4	$M(C_2H_6)^+$	38	32	28	35	19
			C_2H_6	$M(C_2H_4)^+$	tr^e	4			
			C_3H_6	$M(CH_4)^+$				3	
i-C_4H_{10}	105	152	H_2	$M(C_4H_8)^+$	50	69	86	17	
			$2H_2$	$M(C_4H_6)^+$	37	16	9	66	86
			CH_4	$M(C_3H_6)^+$	tr^e	1			
			CH_4,H_2	$M(C_3H_4)^+$	tr^e	1		5	
			C_2H_4	$M(C_2H_6)^+$	12	13	5	12	14
n-C_5H_{12}	172	429	H_2	$M(C_5H_{10})^+$	23	32	19	4	
			$2H_2$	$M(C_5H_8)^+$	26	7	8	34	75
			$3H_2$	$M(C_5H_6)^+$	tr^e			6	3
			CH_4	$M(C_4H_8)^+$	1	8	9		
			CH_4,H_2	$M(C_4H_6)^+$	13	13	13	14	5
			C_2H_4	$M(C_3H_8)^+$	27	34	51	12	4
			C_2H_6	$M(C_3H_6)^+$	1	1		16	3
			C_2H_6,H_2	$M(C_3H_4)^+$		1		2	
			C_3H_6	$M(C_2H_6)^+$	8	4		10	10
			C_3H_8	$M(C_2H_4)^+$		tr^e			
			C_3H_8,H_2	$M(C_2H_2)^+$				2	
i-C_5H_{12}	132		H_2	$M(C_5H_{10})^+$	9				
			$2H_2$	$M(C_5H_8)^+$	64				
			CH_4	$M(C_4H_8)^+$	2				
			CH_4,H_2	$M(C_4H_6)^+$	12				
			C_2H_4	$M(C_3H_8)^+$	4				
			C_3H_6	$M(C_2H_6)^+$	8				
neo-C_5H_{12}	1.5	129	H_2	$M(C_5H_{10})^+$	34	70	71	12	
			CH_4	$M(C_4H_8)^+$		17	14		
			CH_4,H_2	$M(C_4H_6)^+$	31	11	15	65	72
			$CH_4,2H_2$	$M(C_4H_4)^+$	19				
			C_3H_6	$M(C_2H_6)^+$	16	2		23	28
n-C_6H_{14}	232	381	H_2	$M(C_6H_{12})^+$	5	1		1	
			$2H_2$	$M(C_6H_{10})^+$	19	9	22	10	12
			$3H_2$	$M(C_6H_8)^+$	10	4	2	30	53
			$4H_2$	$M(C_6H_6)^+$	12			3	
			CH_4	$M(C_5H_{10})^+$	tr^e	2	4		
			CH_4,H_2	$M(C_5H_8)^+$	9	6		7	6
			$CH_4,2H_2$	$M(C_5H_6)^+$	tr^e			4	2
			C_2H_4	$M(C_4H_{10})^+$	8	20	7	2	2
			C_2H_6	$M(C_4H_8)^+$	11	28	36	14	4
			C_2H_6,H_2	$M(C_4H_6)^+$	12	14	20	8	5
			C_3H_6	$M(C_3H_8)^+$	11	14	9	6	7
			C_3H_8	$M(C_3H_6)^+$	tr^e			6	4
			C_4H_8	$M(C_2H_6)^+$	2			8	3
			C_4H_{10}	$M(C_2H_4)^+$				1	
			C_4H_{10},H_2	$M(C_2H_2)^+$					2

^{a}Reaction cross sections measured at a center-of-mass collision energy of approximately 0.25 eV. ^{b}Reference 1. ^{c}Reference 9. ^{d}No reaction observed. ^{e}Trace amount of this product observed (less than 1%). ^{f}Some $Gd(Cd_4)^+$ product is observed in the reaction with C_3D_3 although large changes in product distributions on deuteration (and the GdO^+ product) make it impossible to estimate the amount of $Gd(CH_4)^+$ formed in the reaction with C_3H_8.

The deuterated products are observed to be about as intense as the $Gd(C_2H_4)^+$ product. The overall product distributions are dependent on the extent of deuteration, and it is thus difficult to estimate the amount of $GdCH_4^+$ formed in reaction of C_3H_8. There are several possible structures, I–III, for the $Gd(CH_4)^+$ product.

$Gd^+ \cdots H\text{-}CH_3$

I

$H\text{-}Gd^+\text{-}CH_3$

II

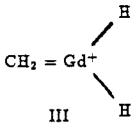

III

Formation of methane and ethylene from propane is endothermic by 19 kcal/mol. We can estimate the interaction energy of Gd^+ and methane. An estimate for the Gd^+ 6s orbital radius is 2.14 Å (as mentioned earlier for Eu^+). For second row metal hydrides, the metal–hydrogen bond length in a covalent bond is about 0.17 Å shorter than this.[12] Coupling this shortest Gd^+–H distance with the C–H bond distance (0.94 Å)[22] gives a minimum

---

(22) Herzberg, G. *Molecular Spectra and Molecular Structure. III. Electronic Spectra of Polyatomic Molecules*, Van Nostrand-Reinhold: New York, 1966.

Table V. Product Distributions in the Reactions of Gd^+ and Sc^+ with Deuterium-Labeled Alkanes

	product distribution (%)					
	propane-*2,2-d*$_2$		2-methyl-propane-*2-d*$_1$		*n*-butane-*1,1,1,4,4,4-d*$_6$	
neutral(s) lost	Gd^{+a}	Sc^{+b}	Gd^{+a}	Sc^{+b}	Gd^{+a}	Sc^{+b}
H_2	26.6	21	30.2	41	2.3	
HD	25.8	33	13.2	27	26.4	38
$2H_2$ (D_2)	7.0	2	26.0	10	1.8	4
H_2 + HD	8.6	3	16.7	6	1.8	
2HD (H_2 + D_2)	2.3	2			15.9	13
HD + D_2			1.1			
$2D_2$			0.5			
CH_4		17				7.0
CH_3D		12				6.2
C_2H_4	6.3		6.2	5	27.5	28
C_2H_3D	14.1	3	7.7	11	4.9	3
$C_2H_2D_2$	*e*	7			1.8	3
C_2HD_3					13.3	8
C_2D_4					0.6	3

[a] Distributions measured at a collision energy of ~0.25 eV. [b] Distributions measured at a collision energy of ~0.5 eV, ref 1. [e] Information about the formation of $Gd(CH_4)^+$ is obscured by the presence of GdO^+.

interaction distance of ~3 Å. Ion induced dipole interaction energies are given by:

$$V(r) = -\frac{e^2\alpha}{2R^4} = -\frac{166\alpha}{{R_0}^4}\ \text{kcal/mol} \qquad (3)$$

where R_0 is the internuclear separation in Å, α is the ligand polarizability in Å^3, and e is the unit charge of the electron.[23] Using the methane polarizability[24] of 2.60 Å^3, the interaction energy is calculated to be only a little over 5 kcal/mol, effectively ruling out structure I (bonding interaction between the metal ion and H could lower the energy slightly). For structure III to be feasible, the strength of two metal–hydrogen bonds plus the metal–methylene bond would have to be over 222 kcal/mol.[25] Considering that Gd^+ has only two non-f valence electrons to bond to the three species, this is highly unlikely. Thus, we feel that the $Gd(CH_4)^+$ species is a hydrido-methyl complex. The presence of this product at low energy gives an estimate for the sum of the Gd^+–H and Gd^+–CH_3 bonds. The process of producing C_2H_4, H, and CH_3 from propane is endothermic by 124.5 kcal/mol. The sum of the two σ bonds must be greater than or equal to this value.

b. *n*-Butane and 2-Methypropane. Figure 2 shows the reactions cross sections as a function of collision energy (at low interaction energies) for the reaction of Gd^+ with *n*-butane. The cross sections show the general behavior for exothermic reactions, decreasing as the collision energy increases. In experiments of Tolbert and Beauchamp on the reactions of Sc^+ with alkanes,[1] it was shown that Sc^+ forms products that involve σ bonding two alkyl groups to the metal in addition to the normal metal–olefin products seen with other metals. This same process has also recently been seen with the other group 3 metal ions Y^+ and La^+.[9] The reaction products for the reaction of Gd^+ with *n*-butane and 2-methylpropane (the distributions for 2-methylpropane are shown in parentheses) are shown in eq 4–6. As with Sc^+, Y^+, and La^+,

$$Gd^+ + C_4H_{10} \xrightarrow{34\%(50\%)} Gd(C_4H_8)^+ + H_2 \qquad (4)$$

$$\xrightarrow{27\%(37\%)} Gd(C_4H_6)^+ + 2H_2 \qquad (5)$$

$$\xrightarrow{38\%(12\%)} Gd(C_2H_6)^+ + C_2H_4 \qquad (6)$$

a product is seen with the general formula $M(C_2H_6)^+$ which, for

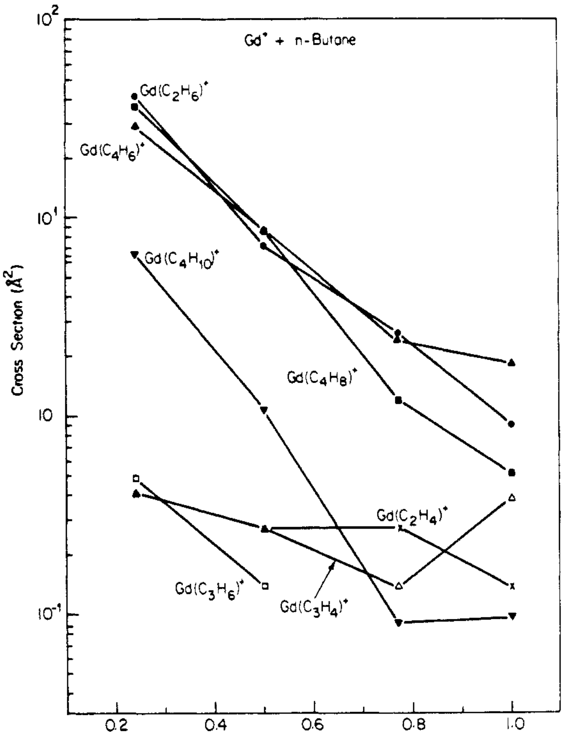

Figure 2. Low-energy products in the reaction of Gd^+ with *n*-butane. The product reaction cross sections are plotted as a function of the center-of-mass collision energy between the metal ion and neutral.

Sc^+, has been shown to be a dimethyl species. As with propane, reaction with deuterium-labeled *n*-butane also shows a very small amount of the hydrido-methyl product (although this product appears to be much less important for the butane case). The other major products observed correspond to loss of one and two molecules of H_2.

With observation of the $Gd(CH_4)^+$ product in the reaction of propane, it is not surprising that "dialkyl" products are also observed with butane and the higher alkanes. As has been pointed out for other metals, the $Gd(C_2H_6)^+$ product could have several possible structures (IV–VI). Structures V and VI were ruled

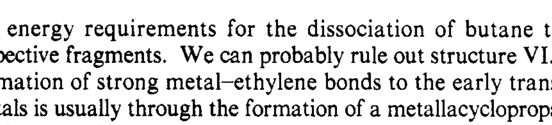

IV V VI

out for Sc^+ because of energy considerations. Equations 7–9 show

$$C_4H_{10} \longrightarrow 2CH_3 + C_2H_4 \qquad \Delta H^\circ = 113.0\ \text{kcal/mol} \qquad (7)$$

$$\longrightarrow H + C_2H_5 + C_2H_4 \qquad \Delta H^\circ = 121.6\ \text{kcal/mol} \qquad (8)$$

$$\longrightarrow 2H + 2C_2H_4 \qquad \Delta H^\circ = 159.5\ \text{kcal/mol} \qquad (9)$$

the energy requirements for the dissociation of butane to the respective fragments. We can probably rule out structure VI. The formation of strong metal–ethylene bonds to the early transition metals is usually through the formation of a metallacyclopropane.[26] With the hydrogen atoms bound to the metal through the two valence electrons, none are left over for bonding to the C_2H_4 fragment and formation of the metallacycle. Structures IV and V are probably both possible from an energetic standpoint. Table V gives the product distributions seen for reaction with butane-*1,1,1,4,4,4-d*$_6$ and 2-methylpropane-*2-d*$_2$. The major neutrals lost giving the dialkyl-type product are C_2H_4 and C_2HD_3 for *n*-butane and C_2H_4 and C_2H_3D for 2-methylpropane. Schemes I and II

---

(23) Benson, S. W. *Thermochemical Kinetics*; Wiley: New York, 1976.

(24) Chan, S. C.; Rabinovitch, B. S.; Bryant, J. T.; Spicer, L. D.; Fujimoto, T.; Lin, Y. N.; Pavlou, S. P. *J. Phys. Chem.* **1970**, *74*, 3160.

(25) Unless otherwise noted, thermochemical values for radicals and carbenes are taken from: (a) Wagman, D. D.; Evans, W. H.; Parker, V. B.; Schumm, R. H.; Halow, I.; Bailey, S. M.; Churney, K. L.; Nuttal, R. L. *J. Phys. Chem. Ref. Data* **1982**, *11*, Suppl. 2. (b) McMillen, D. F.; Golden, D. M. *Annu. Rev. Phys. Chem.* **1982**, *33*, 493.

(26) (a) Steigerwald, M. L.; Goddard, W. A., III *J. Am. Chem. Soc.* **1985**, *107*, 5027. (b) Periana, R. A.; Bergman, R. G. *J. Am. Chem. Soc.* **1986**, *108*, 7346.

Scheme I

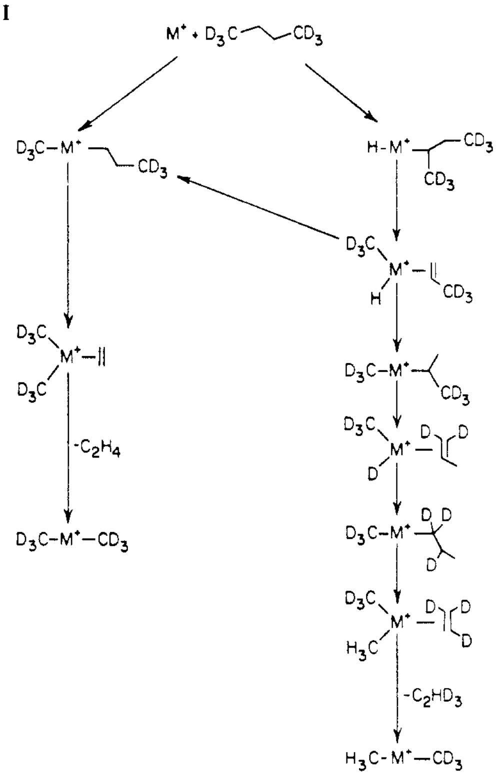

Scheme II

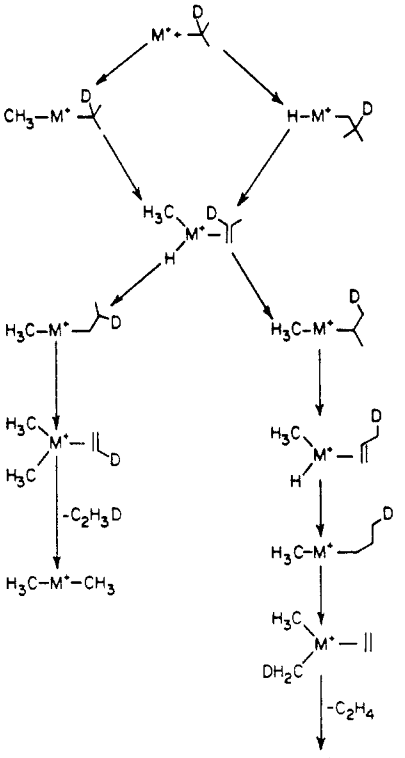

Scheme III

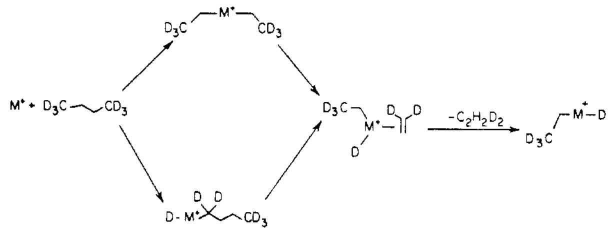

Scheme IV

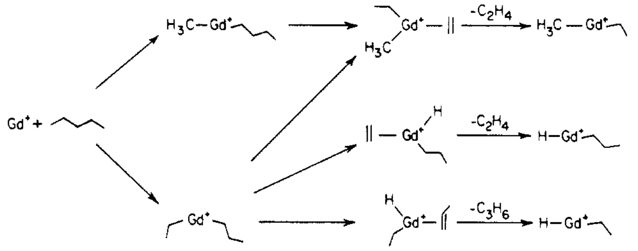

(where $M^+ = Gd^+$) show possible mechanisms (including both C–H and C–C insertion processes) for the formation of the major products for the two neutrals. The products seen to be most abundant can be produced in very straightforward mechanisms. The second major product in both cases is produced by scrambling of the hydrogens. Scheme III (with $M^+ = Gd^+$) shows possible mechanisms for production of a hydrido-ethyl complex from butane. This results in the loss of $C_2H_2D_2$ which is seen as only a minor product in the spectra. Thus, as for Sc^+, the $Gd(C_2H_6)^+$ product is probably the dimethyl species. We will call products of this sort "dialkyl" products although it should be kept in mind that the hydrido-alkyl structures are also possible. With the larger alkanes, a larger number of possible structures exist and we will not attempt to detail them all. Comparison of *n*-butane to 2-methylpropane indicates that the amount of the dialkyl product observed for *n*-butane is greater. Formation of $Gd(C_2H_6)^+$ from 2-methylpropane is uphill 2 kcal/mol compared to the similar process with *n*-butane. This would place a lower limit on the sum of the two metal–carbon σ bonds of 115 kcal/mol.

c. *n*-Pentane, 2-Methylbutane, and 2,2-Dimethylpropane. The major products seen in the reaction of Gd^+ with *n*-pentane are shown in eq 10–16. Again, elimination of one and two molecules

$$Gd^+ + \underline{n}\text{-}C_5H_{12} \xrightarrow{23\%(9\%)} Gd(C_5H_{10})^+ + H_2 \qquad (10)$$

$$\xrightarrow{26\%(64\%)} Gd(C_5H_8)^+ + 2H_2 \qquad (11)$$

$$\xrightarrow{2\%(3\%)} Gd(C_4H_8)^+ + CH_4 \qquad (12)$$

$$\xrightarrow{13\%(12\%)} Gd(C_4H_6)^+ + CH_4 + H_2 \qquad (13)$$

$$\xrightarrow{27\%(4\%)} Gd(C_3H_8)^+ + C_2H_4 \qquad (14)$$

$$\xrightarrow{1\%} Gd(C_3H_6)^+ + C_2H_6 \qquad (15)$$

$$\xrightarrow{8\%(8\%)} Gd(C_2H_6)^+ + C_3H_6 \qquad (16)$$

of H_2 accounts for a significant percentage of the products although other unsaturated products such as Gd^+–butadiene are also seen arising from elimination of both methane and hydrogen. The other major products are dialkyl products. With the lengthening of the alkane chain, two dialkyls are seen, $Gd(C_3H_8)^+$ and $Gd(C_2H_6)^+$. The process of forming CH_3, C_2H_5, and C_2H_4 from *n*-pentane costs 109 kcal/mol, while forming two methyl groups and propene requires 110 kcal/mol. The energy requirements of both processes are just slightly less than forming two methyl groups and ethylene from *n*-butane.

The product percentages for the Gd^+ reaction with 2-methylbutane are shown in parentheses in eq 10–16 for comparison with *n*-pentane. The major differences between the two are the large increase in double dehydrogenation and decrease in $Gd(C_3H_8)^+$ on changing the neutral to 2-methylbutane. Insertion of the metal into a C–C bond provides the most straightforward mechanism for formation of the dialkyl-type products, although mechanisms involving initial C–H insertion (involving more extensive rearrangement) can also be drawn. Schemes IV and V show possible mechanisms for the reactions with *n*-pentane and 2-methylbutane depending upon which C–C bond is initially cleaved. We see that for 2-methylbutane, formation of $Gd(C_3H_8)^+$ would necessarily call for initial insertion into the C_2–C_3 bond, the most sterically hindered C–C bond of the molecule. Insertion into the other C–C bonds leads to the $Gd(C_2H_6)^+$ product. For *n*-pentane, insertion into the C_1–C_2 bond leads to $Gd(C_3H_8)^+$ while insertion into the other C–C bond can lead to both products. It is normally assumed that the larger alkyl groups form stronger bonds because of better stabilization of the metal positive charge.

Table VI. Product Distributions for the Reactions of Gd^+ and Group 3 M^+ with Cycloalkanes

				relative product intensities (%)			
					FTMS[b]		
alkane	total reaction cross section ($Å^2$)[a] Gd^+	neutral(s) lost	product ion	ion beam Gd^+	Sc^+	Y^+	La^+
cyclopropane	62	H_2	$M(C_3H_4)^+$	93	97	100	31
		CH_4	$M(C_2H_2)^+$	3	3		
		C_2H_4	$M(CH_2)^+$	4			69
cyclobutane	133	H_2	$M(C_4H_6)^+$	62	27	30	7
		$2H_2$	$M(C_4H_4)^+$	31	41	28	81
		CH_4	$M(C_3H_4)^+$			4	
		C_2H_2	$M(C_2H_6)^+$	1			
		C_2H_4	$M(C_2H_4)^+$	3	16		
		C_2H_6	$M(C_2H_2)^+$	3	16	38	12
cyclopentane	202	H_2	$M(C_5H_8)^+$	1			
		$2H_2$	$M(C_5H_6)^+$	99	100	100	100
cyclohexane	203	$2H_2$	$M(C_6H_8)^+$	9	11		
		$3H_2$	$M(C_6H_6)^+$	91	89	100	100

[a] Reaction cross sections measured at a center-of-mass collision energy of approximately 0.25 eV. [b] Reference 9.

Scheme V

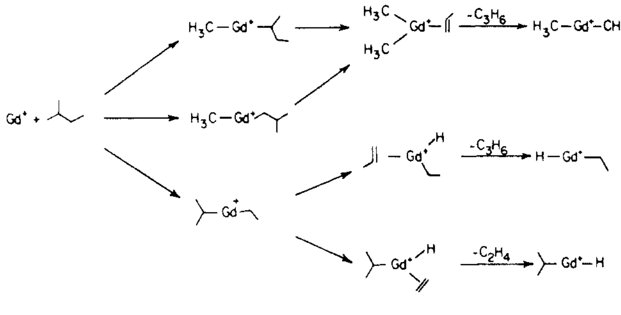

This is a possible explanation for the predominance of the heavier product with *n*-pentane.

An even more drastic change is seen when 2-methylbutane is replaced with 2,2-dimethylpropane. The differences in reaction cross section for the three isomers are (at a collision energy of 0.25 eV) 171.7 $Å^2$ for *n*-pentane, 132.0 $Å^2$ for 2-methylbutane, and 1.5 $Å^2$ for 2,2-dimethylpropane. Thus, the reactivity of Gd^+ with 2,2-dimethylpropane is very low. Dehydrogenation of butane-*1,1,1,4,4,4-d*$_6$ by Sc^+ shows mostly loss of HD. This coupled with the facile dehydrogenation of 2,2-dimethylpropane and the strong σ bonds formed by Sc^+ led to the proposal that the dehydrogenation was by a 1,3 process forming a metallacyclobutane product. Gd^+ also dehydrogenates labeled butane to give predominantly HD loss. However, the unreactivity with 2,2-dimethylpropane tends to indicate that the dehydrogenation process is by a 1,2 mechanism rather than the 1,3 mechanism evidenced by Sc^+. The studies on the reactivity of Y^+ and La^+ also suggest that the 1,3 dehydrogenation is less important for these metals as well.

d. *n*-Hexane. The reaction products observed in the reaction of Gd^+ with *n*-hexane are given in Table IV. The distribution is fairly evenly spread between 10 major products with several minor products also seen. Dehydrogenation products account for almost 50% of the reaction. Elimination of from one to four molecules of H_2 are seen, the latter possibly forming a complex between Gd^+ and benzene. If this is occurring, the energetics yield a lower bound of 60 kcal/mol for the Gd^+–benzene interaction energy. Dialkyl products are again in evidence including $Gd(C_4H_{10})^+$, $Gd(C_3H_8)^+$, and $Gd(C_2H_6)^+$. The dialkyl products decrease, as a percentage of the overall product distribution, as the size of the reacting alkane increases and the number of competing pathways increases.

Reaction of Gd^+ with Cycloalkanes. Table VI lists the reaction products, product distributions, and cross sections for the reactions between Gd^+ and the C_3–C_6 cycloalkanes. The product distributions from FTMS studies of Sc^+, Y^+, and La^+ are also contained in Table VI for comparison with the present results.

a. Cyclopropane and Cyclobutane. The reaction of Gd^+ with cyclopropane yields the products shown in Table VI. Elimination of H_2 is by far the major reaction pathway. CID experiments on the $M(C_3H_4)^+$ products in the reactions of Y^+ and La^+ with cyclopropane show these products to be very similar to those formed from propane and propene, suggesting that the ring has been opened. The C–C bond is clearly the weakest bond in the molecule while the C–H bonds of cyclopropane are exceptionally strong (106 kcal/mol).[25b] The pathway of choice would thus seem to be insertion into one of the ring C–C bonds. Condensed-phase experiments by Periana and Bergman[26] indicate that the reaction of $Cp^*(L)Rh$ ($Cp^* = \eta^5\text{-}C_5Me_5$; $L = PMe_3$) with cyclopropane proceeds first through oxidative addition of a cyclopropyl-H bond to the metal and then intramolecular rearrangement gives the metallacyclobutane. Either mechansm would result in the cleavage of the cyclopropane ring. Two β-H transfers and reductive elimination of H_2 would then yield the product. Small amounts of other ring cleavage products, $Gd(C_2H_2)^+$ and $GdCH_2^+$, are also seen. Formation of the metal–methylene product requires a metal–carbon double bond strength which is greater than 93 kcal/mol.

Hydrogen loss products are the principal reaction products observed in the reaction with cyclobutane, although small amounts of C–C bond cleavage products are also seen (eq 17–21). A trace

$$Gd^+ + c\text{-}C_4H_8 \xrightarrow{62\%} Gd(C_4H_6)^+ + H_2 \tag{17}$$

$$\xrightarrow{31\%} Gd(C_4H_4)^+ + 2H_2 \tag{18}$$

$$\xrightarrow{1\%} Gd(C_2H_6)^+ + C_2H_2 \tag{19}$$

$$\xrightarrow{3\%} Gd(C_2H_4)^+ + C_2H_4 \tag{20}$$

$$\xrightarrow{3\%} Gd(C_2H_2)^+ + C_2H_6 \tag{21}$$

amount of methane loss is also observed in the reaction. As with cyclopropane, these products probably result from initial insertion into one of the C–C bonds. H_2 loss then occurs through successive β-H transfers and reductive elimination. Further elimination of H_2 yields the $Gd(C_4H_4)^+$ product. Both of these hydrogen loss products could be produced without ring cleavage through C–H insertion and successive hydrogen transfer and elimination. The C–H bond strength is not excessively strong (96.5 kcal/mol) as it is in cyclopropane. The reactions of Y^+ and La^+ have been proposed[9] to differ in that Y^+ is thought to initially cleave the ring while La^+ is thought to interact with the cyclobutane C–H bonds. The C–C bond cleavage products can be thought of as coming from initial formation of a metallacyclopentane and then symmetric ring cleavage followed by elimination of neutral product molecules.

b. Cyclopentane and Cyclohexane. No ring cleavage products are observed in the reaction of Gd^+ or the three group 3 metal ions with cyclopentane and cyclohexane. Dehydrogenation is the only process involved in these reactions, with the major product ions arising from loss of two (cyclopentane) and three (cyclohexane) molecules of hydrogen. These are believed to correspond to Gd^+–cyclopentadiene and Gd^+–benzene complexes. Formation of cyclopentadiene and hydrogen from cyclopentane is endothermic by 50 kcal/mol. This is a lower bound for the binding energy

Table VII. Product Distributions for the Reactions of Gd^+ and Pr^+ with Alkenes

	total reaction cross section (Å^2)[a]				relative product intensities (%)	
alkene	Gd^+	Pr^+	neutral(s) lost	product ion	Gd^+	Pr^+
ethene	44	0.9	H_2	$M(C_2H_2)^+$	100.0	100.0
propene	230	30	H_2	$M(C_3H_4)^+$	99.0	97.7
			CH_4	$M(C_2H_2)^+$	0.6	0.3
			C_2H_4	$M(CH_2)^+$	0.4	2.0
1-butene	406	223	H_2	$M(C_4H_6)^+$	95.5	98.2
			$2H_2$	$M(C_4H_4)^+$	0.7	0.2
			CH_4	$M(C_3H_4)^+$	1.6	0.6
			C_2H_4	$M(C_2H_4)^+$	0.3	0.2
			C_2H_6	$M(C_2H_2)^+$	1.8	0.5
			C_3H_6	$M(CH_2)^+$	0.1	0.3
1-pentene	454	273	H_2	$M(C_5H_8)^+$	33.6	85.7
			$2H_2$	$M(C_5H_6)^+$	35.8	9.2
			CH_2	$M(C_4H_8)^+$	0.3	0.1
			CH_4	$M(C_4H_6)^+$	7.8	1.0
			CH_4,H_2	$M(C_4H_4)^+$	0.2	
			C_2H_2	$M(C_3H_8)^+$	0.1	
			C_2H_4	$M(C_3H_6)^+$	1.7	0.9
			C_2H_6	$M(C_3H_4)^+$	20.0	2.7
			C_3H_4	$M(C_2H_6)^+$	0.1	
			C_3H_6	$M(C_2H_4)^+$	0.1	0.1
			C_3H_8	$M(C_2H_2)^+$	0.3	0.1
			C_4H_8	$M(CH_2)^+$		0.2
1-hexene	452	167	H_2	$M(C_6H_{10})^+$	7.3	21.2
			$2H_2$	$M(C_6H_8)^+$	62.1	65.3
			$3H_2$	$M(C_6H_6)^+$	5.6	2.0
			CH_2	$M(C_5H_{10})^+$	0.2	
			CH_4	$M(C_5H_8)^+$	1.1	0.5
			CH_4,H_2	$M(C_5H_6)^+$	9.2	2.8
			$CH_4,2H_2$	$M(C_5H_4)^+$	0.1	
			C_2H_4	$M(C_4H_8)^+$	0.8	0.5
			C_2H_6	$M(C_4H_6)^+$	10.0	5.9
			C_3H_6	$M(C_3H_6)^+$	0.5	0.4
			C_3H_8	$M(C_3H_4)^+$	2.0	1.1
			C_4H_6	$M(C_2H_6)^+$	1.0	0.1
			C_4H_8	$M(C_2H_4)^+$		0.1
			C_4H_{10}	$M(C_2H_2)^+$	0.1	
			C_5H_{10}	$M(CH_2)^+$		0.1
cyclohexene	313	340	H_2	$M(C_6H_8)^+$	0.4	0.5
			$2H_2$	$M(C_6H_6)^+$	99.2	99.5
			C_6H_8	$M(H_2)^+$	0.4	

[a] Reaction cross sections measured at a center-of-mass collision energy of approximately 0.25 eV.

to Gd^+. It is noted about that the Gd^+–benzene may be bound by at least 60 kcal/mol. Formation of benzene from cyclohexane is endothermic by 49 kcal/mol, so that formation of Gd^+–benzene is consistent with the earlier result.

Reactions of Gd^+ and Pr^+ with Alkenes. Activation of C–C and C–H bonds in alkanes requires formation of two strong σ bonds by the metal. In contrast, activation of C–H and C–C bonds in alkenes is enhanced by the interaction of the alkene π system with the metal ion. First row metals are seen to bind alkenes with a bond energy on the order of 40–50 kcal/mol.[27] The need for strong metal σ bonding in the inserted product is thus not as great. The reactivity of Pr^+ with alkenes and not with alkanes is an example of this. Eu^+, on the other hand, has an extremely stable, half-filled f shell (f^7). We have tested the reactivity of Eu^+ with cyclohexene, a fairly reactive alkene, and observed only adduct formation and no elimination products. Table VII presents the reaction data for the reaction of Gd^+ and Pr^+ with cyclohexene and the linear alkenes from ethene to 1-hexene.

a. Ethene and Propene. Gd^+, as was discussed earlier, doubly dehydrogenates ethane. It is thus expected that dehydrogenation of ethene will take place and this is indeed what is observed. The same process is also seen for Pr^+, although the extremely low efficiency (σ_{rxn} = 0.9 Å^2 at a collision energy of 0.25 eV). Three products are observed in the reaction of propene with Gd^+ (Pr^+), eq 22–24. The major product in both cases is elimination of one

$$M^+ + C_3H_6 \xrightarrow{99\%(97.7\%)} M(C_3H_4)^+ + H_2 \tag{22}$$

$$\xrightarrow{0.6\%(0.3\%)} M(C_2H_2)^+ + CH_4 \tag{23}$$

$$\xrightarrow{0.4\%(2.0\%)} M(CH_2)^+ + C_2H_4 \tag{24}$$

molecule of H_2. The process can take place via interaction of the metal ion with the weakest C–H bonds in the molecule, the allylic C–H bonds. After formation of a metal–hydrido–allyl complex, hydrogen transfer and H_2 elimination yields a metal–allene product. The presence of the MCH_2^+ product at low energy provides an estimate of the strength of the metal–carbon double bond of greater than or equal to 101 kcal/mol.

Scheme VI

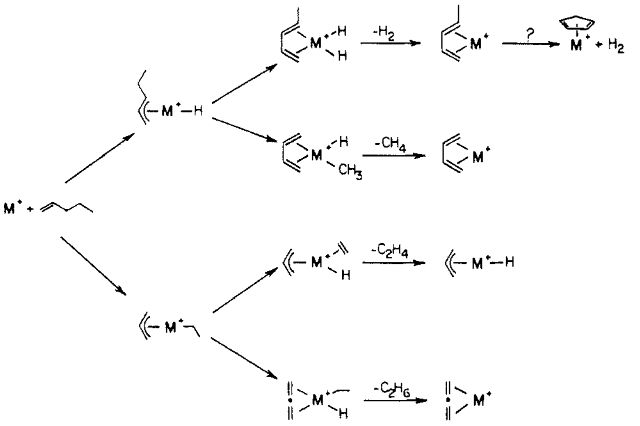

The formation of $PrCH_2^+$ from propene and cyclopropane, the first being exothermic and the second appearing endothermic, poses a dilemma. Exothermic production from propene requires a bond strength of greater than 101 kcal/mol while endothermic production from cyclopropane would indicate that the bond energy is less than 93 kcal/mol. Two explanations exist for the discrepancy between the two results. First, the production of $PrCH_2^+$ from propene could be due to reaction of excited-state Pr^+. Secondly, if we look more closely at the reactions of the two systems we see that there is another reaction product, $Pr(C_3H_4)^+$, that the two have in common. Again, the product is formed in an exothermic reaction with propene and a seemingly endothermic reaction with cyclopropane. The formation of C_3H_4 and H_2 from propene is 7.9 kcal/mol more endothermic than formation from cyclopropane. If the reaction with cyclopropane does not indeed proceed via ring cleavage and β-H transfer, then the two processes proceed through a common intermediate. This indicates that there is possibly a thermodynamic barrier on the potential surface for interaction of Pr^+ with cyclopropane. The exact nature of the metal–methylene bonding is not known at this time.

b. 1-Butene and 1-Pentene. As the size of the alkene increases, the number of products observed also increases. Seven products are observed in the reaction of Gd^+ with 1-butene and 13 with 1-pentene. Pr^+ exhibits slightly lower reactivity and slightly fewer products. The product intensities for those products with abundances of 0.1% or larger are shown in Table VII. Dehydrogenation is again the major reaction pathway, representing over 95% of the product intensity for both metals in the reaction with 1-butene. Minor amounts of carbon–carbon bond cleavage products are also observed.

Scheme VI shows possible reaction mechanisms accounting for the major products observed with 1-pentane. These involve insertion of the metal into either an allylic C–H or C–C bond. C–C insertion leads to the $M(C_3H_6)^+$ and $M(C_3H_4)^+$ products while C–H inserion would lead to the dehydrogenation products and also loss of CH_4.

c. 1-Hexene and Cyclohexene. Eighteen different products are observed at low energy in the reaction of Gd^+ with 1-hexene, while 13 are observed in the reaction involving Pr^+; 75 and 88% of the product abundance, for Gd^+ and Pr^+, respectively, is due to single

---

(27) (a) Aristov, N.; Armentrout, P. B. *J. Am. Chem. Soc.* **1986**, *108*, 1806. (b) Hanratty, M. A.; Beauchamp, J. L.; Illies, A. J.; van Koppen, P.; Bowers, M. T. *J. Am. Chem. Soc.*, preceding paper in this issue.

Table VIII. Product Distributions for the Reactions of Gd^+ and Pr^+ with Oxygen-Containing Compounds

alkene	total reaction cross section (Å²)[a] Gd⁺	total reaction cross section (Å²)[a] Pr⁺	neutral(s) lost	product ion	relative product intensities (%) Gd⁺	relative product intensities (%) Pr⁺
nitric oxide	4.8	16	N	MO^+	100.0	100.0
formaldehyde	86	43	CH_2	MO^+	29.1	100.0
			CO	MH_2^+	70.9	
acetaldehyde	614	319	H_2	$M(C_2H_2O)^+$	1.4	
			C_2H_2	$M(OH_2)^+$	0.2	
			C_2H_4	MO^+	98.1	100.0
			CO	$M(CH_4)^+$	0.3	
acetone	352	385	H_2	$M(C_3H_4O)^+$	2.4	
			CH_3	$M(C_2H_3O)^+$	0.1	
			CH_4	$M(C_2H_2O)^+$	0.3	
			CO	$M(C_2H_6)^+$	0.2	
			C_3H_4	$M(OH_2)^+$	0.5	0.1
			C_3H_6	MO^+	96.5	99.9

[a] Reaction cross sections measured at a center-of-mass collision energy of approximately 0.25 eV.

and multiple dehydrogenation processes. Smaller amounts are seen in chain cleavage processes. Again, the major products can be predicted by mechanisms involving initial insertion into allylic bonds followed by β-H or β-alkyl transfer and reductive elimination of the neutral species. We will not attempt to account for the processes producing all 18 products.

The reactions of cyclohexene are quite a contrast to those of 1-hexene. A total of only three low energy products are seen. Both Gd^+ and Pr^+ doubly dehydrogenate cyclohexene to produce M^+–benzene, a product which accounts for over 99% of the total product distribution. In the reaction with Gd^+, an endothermic process is also seen with a threshold at very low energy. This process produces GdH_2^+ and either cyclohexadiene or benzene and hydrogen. The latter process is the most energetically favorable. It is uphill 125 kcal/mol to produce benzene, hydrogen, and two H atoms. The threshold for production of GdH_2^+ appears to be less than 0.25 eV (5.8 kcal/mol). This would put an upper limit on the sum of the two Gd^+–H σ bonds somewhere between 119 and 125 kcal/mol.

Reaction of Gd⁺ and Pr⁺ with Oxygen-Containing Compounds. The two ions have been reacted with nitric oxide, formaldehyde, acetaldehyde, and acetone. As mentioned earlier, Gd^+ readily reacts with any O_2 in the system. Pr^+ is also seen to form the oxide when any oxygen is present. Table VIII lists the products observed at low collision energy for these systems. The principal product in almost all of the reactions (eq 25–28) is MO^+. Small

$$M^+ + NO \longrightarrow MO^+ + N \qquad (25)$$

$$M^+ + (CH_3)_2CO \longrightarrow MO^+ + C_3H_6 \qquad (26)$$

$$M^+ + CH_3CHO \longrightarrow MO^+ + C_2H_4 \qquad (27)$$

$$M^+ + CH_2O \longrightarrow MO^+ + {:}CH_2 \qquad (28)$$

amounts of other products are also seen. In the reaction with acetone, both metal ions produce $M(OH_2)^+$ with the loss of C_3H_4. Other products observed in the reaction of Gd^+ with acetone involve elimination of H_2, CH_3, CH_4, and CO. Elimination of CO yields the metal–dimethyl ion (the sum of the two bonds must be greater than or equal to 95.7 kcal/mol). Gd^+ reacts with acetaldehyde to give, in addition to GdO^+, $Gd(C_2H_2O)^+$, $Gd(OH_2)^+$, and $Gd(CH_4)^+$. The presence of a small amount of the hydrido-methyl species was determined using CH_3CDO and CD_3CDO to distinguish this product from the oxide and water complexes. Formation of the hydrido-methyl complex requires that the sum of the metal–hydrogen and metal–methyl bonds be greater than or equal to 100.5 kcal/mol. The other important nonoxide product observed in these reactions is GdH_2^+, formed in the reaction with formaldehyde. The large reaction cross section indicates that the two metal–hydrogen bonds are much stronger than the 103.7 kcal/mol necessary for formation of the product.

Table IX. Heats of Dissociation for Gaseous Oxygen-Containing Molecules

reaction	$\Delta H°_{298}$ (kcal/mol)
$O_2 \rightarrow O + O$	117
$NO \rightarrow O + N$	151
$(CH_3)_2CO \rightarrow O + H_2C{=}CHCH_3$	116
$\rightarrow O + {:}C(CH_3)_2$	174
$CH_3CHO \rightarrow O + H_2C{=}CH_2$	112
$\rightarrow O + {:}CHCH_3$	177
$CH_2O \rightarrow O + {:}CH_2$	179

[a] Individual heats of formation from ref 21, 25, and 28.

This is in keeping with the earlier result of ~120 kcal/mol from the endothermic formation of this product from cyclohexane. GdH_2^+ is therefore stable with respect to reductive elimination of H_2.

In the reaction of Gd^+ with acetone and acetaldehyde several secondary reactions of the product oxide were observed. Collisions of the abundant GdO^+ product at higher pressures led to formation of secondary reaction products, the primary one being the dehydration of the neutral to give $PdO(OH_2)^+$. One other secondary product, $Gd(O_2)^+$, is also observed.

For thermodynamic analysis, the neutral decomposition pathways and energetics for production of O atom from the various species are given in Table IX. Reaction with formaldehyde, reaction 28, is seen for both metal ions. For a reaction to take place between M^+ and CH_2O to produce MO^+, the M^+–O bond dissociation energy must be greater than or equal to 179 kcal/mol. Reaction with acetaldehyde and acetone can thus produce either the neutral alkenes or the corresponding methyl and dimethyl carbene. Metal ions show considerable diversity in their reactions with acetone depending upon the strength of the metal oxide bond. The group 8–10 metal ions form much weaker bonds to oxygen.[29] The group 8–10 metals of the first row (Fe^+, Co^+, and Ni^+),[30] along with Pd^+,[7] react to give primarily the metal–dimethyl product, $M(CH_3)_2^+$, with smaller amounts of the metal carbonyl, MCO^+. Group 8–9 metals of the second row (Ru^+ and Rh^+)[7] yield $M(CH_2O)^+$ and $M(C_2H_4)^+$ products as well as $M(CH_3)_2^+$ and MCO^+. Mo^+ reacts with acetone predominantly by a dehydrogenation pathway[31] to give presumably $Mo(CO)(C_2H_4)^+$. Sc^+, on the other hand, with an oxide bond energy of about 159 kcal/mol, behaves similarly to Pr^+, producing only the oxide product.[1] $D(Sc^+–O)$, however, is not large enough to produce the oxide from formaldehyde because of the high heat of formation of methylene.

The present results for $D(Pr^+–O)$ and $D(Gd^+–O)$, giving a lower limit of 179 kcal/mol, compare very well with calculations of the bond energies from known quantities for neutral MO.[32] Using the MO bond energies of 177.6 ± 4.0 and 169.7 ± 3.0 kcal/mol for Pr^+ and Gd^+, respectively, the MO ionization potentials of 4.90 ± 0.1 and 5.75 ± 0.1 eV, and the metal atom IP's of 5.37 ± 0.1 and 6.24 ± 0.1 eV, one can calculate (using the thermodynamic cycle shown below) the metal oxide cation bond dissociation energies. Values of 188.4 ± 5.2 and 181.0 ± 4.4 kcal/mol are calculated for $D(Pr^+–O)$ and $D(Gd^+–O)$, respectively, slightly

$$\begin{tikzcd}
MO^+ + e^- \arrow[r, "D(M^+-O)"] & M^+ + O + e^- \\
MO \arrow[u, "IP(MO)"] \arrow[r, "D(M-O)"'] & M + O \arrow[u, "IP(M)"']
\end{tikzcd}$$

---

(28) The heats of formation of $(CH_3)_2C$ and $(CH_3)HC$ were obtained from: Liu, K.; Parson, J. M. *J. Phys. Chem.* **1979**, *83*, 970.

(29) (a) Armentrout, P. B.; Halle, L. F.; Beauchamp, J. L. *J. Chem. Phys.* **1982**, *76*, 2449. (b) Armentrout, P. B.; Halle, L. F.; Beauchamp, J. L. *J. Am. Chem. Soc.* **1981**, *103*, 6501.

(30) (a) Burnier, R. C.; Byrd, G. D.; Freiser, B. S. *J. Am. Chem. Soc.* **1981**, *103*, 4630. (b) Halle, L. F.; Crowe, W. E.; Armentrout, P. B.; Beauchamp, J. L. *Organometallics* **1984**, *3*, 1694.

(31) Schilling, J. B.; Beauchamp, J. L. *Organometallics*, in press.

(32) (a) Pedley, J. B.; Marshall, E. M. *J. Phys. Chem. Ref. Data* **1983**, *12*, 967. (b) Ackerman, R. J.; Rauh, E. G.; Thorn, R. J. *J. Chem. Phys.* **1976**, *65*, 1027.

greater than the lower limit set by the present experiments. A similar calculation for Eu^+ using D(Eu–O) = 114.5 ± 4.0 kcal/mol, IP(EuO) = 6.48 ± 0.1 eV, and IP(Eu) = 5.68 ± 0.1 eV, yield an EuO^+ bond dissociation energy of 96.1 ± 5.2 kcal/mol, explaining why no EuO^+ product was seen due to background oxygen in the system.

Conclusion

The results presented show that those lanthanide cations which, of necessity, must involve the f electrons in bonding, are unable to activate the C–H or C–C bonds of saturated hydrocarbons. This supports the contention that bonds formed utilizing the f electrons are inherently weak. On the other hand, where two non-f valence electrons are available for use in bonding, the metal ion is very reactive. Gd^+, with a ground state derived from the $4f^75d^16s^1$ configuration, exhibits reactivity similar to that of the group 3 transition metal cations. Product distributions are fairly similar to Sc^+, although more multiple dehydrogenation products are seen for Gd^+. As with Sc^+, Gd^+ is capable of forming two strong σ bonds to carbon and hydrogen. An estimate of the sum of the two bonds in GdH_2^+ is 120 ± 5 kcal/mol. $Gd(CH_3)(H)^+$ is produced in the reaction with propane indicating that the sum of the bonds is around 125 kcal/mol. Although the reactions yielding $Gd(C_2H_6)^+$ yield an estimate of 115 kcal/mol for the sum of the bond energies, it is also likely to be over 120 kcal/mol.

By looking at the electronic states of the other lanthanide cations, one can try to make predictions of reactivity. Ce^+ and Lu^+ are the other two ions with two non-f valence electrons; however, Lu^+ has a closed-shell $f^{14}s^2$ configuration. An $f^{14}d^1s^1$ configuration which would be necessary for bonding is at over 1.5 eV. Ce^+ has two 5d electrons, like La^+, and should be quite reactive in its ground state. The other lanthanide cations only have one non-f valence electron. Except for Tb^+, which has a state at approximately 0.4 eV with a $4f^85d^16s^1$ configuration, the reactive excited states are fairly high in energy and it can be expected that these ions will all be unreactive.

Acknowledgment. We thank the donors of the Petroleum Research Fund, administered by the American Chemical Society, and the National Science Foundation (Grant No. CHE84-07857) for partial support of this work.

Registry No. Eu^+, 15065-79-9; Pr^+, 20193-53-7; Gd^+, 19180-89-3; CH_4, 74-82-8; C_2H_6, 74-84-0; C_3H_8, 74-98-6; n-C_4H_{10}, 106-97-8; i-C_4H_{10}, 75-28-5; n-C_5H_{12}, 109-66-0; i-C_5H_{12}, 78-78-4; neo-C_5H_{12}, 463-82-1; n-C_6H_{14}, 110-54-3; propane-*2,2-d*$_2$, 2875-95-8; 2-methylpropane-*2-d*$_1$, 20717-74-2; n-butane-*1,1,1,4,4,4-d*$_6$, 13183-67-0; cyclopropane, 75-19-4; cyclobutane, 287-23-0; cyclopentane, 287-92-3; cyclohexane, 110-82-7; ethene, 74-85-1; propene, 115-07-1; 1-butene, 106-98-9; 1-pentene, 109-67-1; 1-hexene, 592-41-6; cyclohexene, 110-83-8; nitric oxide, 10102-43-9; formaldehyde, 50-00-0; acetaldehyde, 75-07-0; acetone, 67-64-1.

Thermochemistry of Silaethylene and Methylsilylene from Experiment and Theory

Seung Koo Shin, Karl K. Irikura, J. L. Beauchamp,* and William A. Goddard, III

Contribution No. 7595 from the Arthur Amos Noyes Laboratory of Chemical Physics, California Institute of Technology, Pasadena, California 91125.

Received June 15, 1987

Abstract: Fourier transform ion cyclotron resonance spectroscopy has been used to examine the deprotonation energetics of the methylsilyl cation, $CH_3SiD_2^+$, to yield silaethylene and methylsilylene proton affinities of 205 ± 3 and 215 ± 4 kcal/mol, respectively. These values, combined with the known heat of formation of methylsilyl cation, yield $\Delta H_f{}^\circ{}_{298}(CH_2SiH_2)$ = 43 ± 3 kcal/mol and $\Delta H_f{}^\circ{}_{298}(CH_3SiH)$ = 53 ± 4 kcal/mol. These results are corroborated by ab initio generalized valence bond–configuration interaction calculations which indicate that silaethylene is more stable than methylsilylene by 11.6 kcal/mol, in excellent agreement with the experimental difference (10 ± 3 kcal/mol). The adiabatic ionization potential of methylsilylene is calculated to be 8.22 eV, which is lower than the value of 8.85 eV determined for silaethylene using photoelectron spectroscopy.

The reactivities, structures, and thermochemistry of Si–C double-bonded compounds,[1] silaethylenes, and divalent silicon compounds, silylenes,[2] have been the subject of extensive study, ever since dimethylsilaethylene was first suggested as a reactive intermediate in the pyrolysis of 1,1-dimethylsilacyclobutane.[3] Silaethylene (**1**) and its isomer methylsilylene (**2**) have been

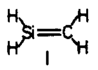
1

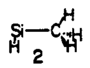
2

isolated in an argon matrix[4] and spectroscopically characterized.[5,6] The interconversion of these two reactive species has been examined to elucidate the isomerization energetics.[5,7] However, no experimental determinations of the heats of formation of these

Table I. Theoretical Predictions of the Relative Stabilities of Silaethylene and Methylsilylene

year	method[a]	ΔE($SiHCH_3$ – SiH_2CH_2) (kcal/mol)	ref
1978	CI/STO-3G//HF/STO-4G	–6.8	*b*
1980	MP2/6-31G*//HF/4-31G	2.1	*c*
1980	CI/DZ+d//HF/DZ	–0.4	*d*
1981	CI(pseudo-pot)/DZ+d	3.5	*e*
1982	CI/DZ+P//HF/DZ+P + Davidson correction	1.7	*f*
1982	CEPA/extended (p+d) //HF/extended (d)	0.6	*g*
1984	CI/6-31G*//HF/6-31G* + Davidson correction	–3.4	*h*
1987	CC-CI/VDZ+P//MP2/6-31G** + zero-point-energy correction	11.6	*i*

[a] Calculational level for total energy/basis sets//calculational level for geometry optimization/basis sets; for example, CI/STO-3G//HF/STO-4G represents the CI level energy calculation with STO-3G basis sets and the HF/STO-4G optimized geometry. For details, see references. [b] Reference a. [c] Reference 8b. [d] Reference 8c. [e] Reference 8d. [f] Reference 1d. [g] Reference 8e. [h] Reference 8f. [i] This work.

---

[1] For recent reviews, see: (a) Raabe, G.; Michl, J. *Chem. Rev.* **1985**, *85*, 419. (b) Bertrand, G.; Trinquier, G.; Mazerolles, P. *J. Organomet. Chem. Libr.* **1981**, *12*, 1. (c) Gusel'nikov, L. E.; Nametkin, N. S. *Chem. Rev.* **1979**, *79*, 529. (d) Schaefer, H. F., III *Acc. Chem. Res.* **1982**, *15*, 283.

[2] Gaspar, P. P. In *Reactive Intermediates*; Jones, M., Moss, R. A., Eds.; Wiley: New York, 1985; Vol. 3, Chapter 9 and earlier volumes.

[3] (a) Nametkin, N. S.; Vdovin, V. M.; Gusel'nikov, L. E.; Zav'yalov, V. I. *Izv. Akad. Nauk SSSR, Ser. Khim.* **1966**, 584. (b) Flowers, M. C.; Gusel'nikov, L. E. *J. Chem. Soc. B* **1968**, 419.

[4] Maier, G.; Mihm, G.; Reisenauer, H. P. *Chem. Ber.* **1984**, *117*, 2351.

[5] (a) Maier, G.; Mihm, G.; Reisenauer, H. P.; Littman, D. *Chem. Ber.* **1984**, *117*, 2369. (b) Rosmus, P.; Bock, H.; Solouki, B.; Maier, G.; Mihm, G. *Angew. Chem., Int. Ed. Engl.* **1981**, *20*, 598.

[6] Auner, N.; Grobe, J. *Z. Anorg. Allg. Chem.* **1979**, *459*, 15.

0002-7863/88/1510-0024$01.50/0